

A Novel Algorithm for Determining Endocardial VT Exit Site from 12-Lead Surface ECG Characteristics in Human, Infarct-Related Ventricular Tachycardia

OLIVER R. SEGAL, M.R.C.P.,* ANTHONY W.C. CHOW, M.D., F.R.C.P.,* TOM WONG, M.R.C.P.,* NICOLA TREVISI, M.D.,† MARTIN D. LOWE, PH.D., M.R.C.P.,‡ D. WYN DAVIES, M.D., F.R.C.P.,* PAOLO DELLA BELLA, M.D.,† DOUGLAS L. PACKER, M.D.,‡ and NICHOLAS S. PETERS, M.D., F.R.C.P.*

From the *Imperial College London and St. Mary's Hospital, London, UK; †Arrhythmia Department, University of Milan, Centro Cardiologico Monzino, Milan, Italy; and ‡Mayo Medical Center, Rochester, Minnesota, USA

New ECG Algorithm for Infarct-Related VT. *Introduction:* Characteristics of the 12-lead ECG during VT are used to guide initial placement of mapping catheters in endocardial ventricular tachycardia (VT) ablation. Previously constructed algorithms for guidance in human infarct-related VT are limited to patients known to have anterior or inferior infarcts only. We hypothesized that 12-lead ECG characteristics could be used to determine VT exit site in patients with all types of infarction of unknown location.

Methods and Results: From noncontact activation maps of 121 LV VT in 51 patients undergoing catheter ablation, VT exit sites were determined and correlated with ECG characteristics according to bundle branch block configuration, limb lead polarity and patterns of precordial R-wave transition. Eight ECG patterns were identified that accounted for 71% of all VT and gave a positive predictive value (PPV) $\geq 70\%$ using the first two criteria. No correlation was found with patterns of R-wave transition. Using these criteria an algorithm was developed, which was then applied prospectively and blinded to a further 17 VT in 11 patients. Of the 15 VT (88%) to which the algorithm predicted an exit site location (with a PPV $\geq 70\%$), 14 VT (93%) were correctly predicted by the algorithm.

Conclusion: This algorithm can be used to predict endocardial LV VT exit site location in patients undergoing catheter ablation of VT without knowledge of or reference to infarct location, and can be applied to patients with posterior and/or multiple sites of infarction. (*J Cardiovasc Electrophysiol*, Vol. 18, pp. 161-168, February 2007)

tachycardia, ventricles, electrocardiography, endocardium, ablation

Introduction

Accurate and rapid localization of the endocardial origin of ventricular tachycardia (VT) circuits is necessary during conventional mapping and catheter ablation of infarct-related VT. Furthermore, described techniques for treating poorly tolerated or noninducible VT by ablating during sinus rhythm, based on voltage or scar mapping with anatomically guided linear ablation, would be enhanced by prior knowledge of the region of origin of ventricular activation during the clinical VT, to help focus the treatment.

There have been two previous attempts at identifying 12-lead ECG characteristics useful in predicting VT exit site region in patients with infarct-related VT. The first al-

gorithm, published by Miller et al.¹ used endocardial contact catheter mapping and, in some cases epicardial mapping during surgery, to determine VT exit site location. Thus, VT generally had to be sustained and hemodynamically stable to enable mapping, the patient population was strictly limited to those with either anterior or inferior sites of infarction, and knowledge of infarct location was required for use of the algorithm.

A refinement of this algorithm developed by Kucher et al.² used left ventricular (LV) endocardial pacing during sinus rhythm to determine ECG features specific for particular LV sites. Again, the patient population was limited to those with anterior and/or inferior sites of infarction, prior knowledge of which was required. Activation sequence mapping to determine VT exit site location was limited to episodes of sustained and hemodynamically stable VT.

In addressing the hypothesis that 12-lead ECG characteristics during VT correlate with exit site location without reference to or knowledge of infarct location, ECG features during VT were correlated with VT exit site location determined by noncontact mapping. Using this approach, which reliably and uniquely locates endocardial exit sites in unstable and nonsustained VT as well as stable VT,³ an algorithm was constructed to predict the region of VT exit site, further verified by successful ablation at sites closely related to the VT exit sites. The algorithm was then tested prospectively and blinded in a separate group of patients at a different center.

Drs. Segal, Peters, and Chow were supported by Project Grant PG/2001030 from the British Heart Foundation. Dr. Packer has a royalty agreement with Endocardial Solutions, Inc., for the mapping system used in this and other studies.

Address for correspondence: Nicholas S. Peters, M.D., F.R.C.P., Waller Cardiac Department, St. Mary's Hospital, Praed Street, London, W2 1NY, UK. Fax: 0044-20-7886-1763; E-mail: n.peters@imperial.ac.uk

Manuscript received 5 June 2006; Revised manuscript received 26 September 2006; Accepted for publication 29 September 2006.

doi: 10.1111/j.1540-8167.2007.00721.x

Methods

Patient Population

Fifty-one unselected patients with remote MI (>6 months) referred for catheter ablation of VT (5 female, age of 63.2 ± 8.1 years [range 44–79], ejection fraction [EF] $33.7 \pm 7.0\%$) were included. The study with the Declaration of Helsinki was approved by the local ethics committee, whose guidelines were followed; and after written informed consent, patients were studied in the postabsorptive state. All antiarrhythmic drugs except amiodarone were withdrawn prior to the study.

Mapping

A percutaneous catheter-mounted mapping system (EnSite 3000, Endocardial Solutions, Inc., St. Paul, MN, USA) was used to produce high-resolution endocardial activation maps of the entire LV and has been described in detail before.³ In brief, a 64 wire, balloon-mounted, multi-electrode array was deployed retrogradely in the LV with two quadripolar/mapping catheters, deployed retrogradely and via transseptal puncture. A standard quadripolar catheter was placed at the right ventricular apex (RVA). Having generated the endocardial geometry, anatomical landmarks established by single-plane fluoroscopy were recorded on the geometry. In patients not in tachycardia at the start of the study, VT induced by programmed stimulation were recorded using the noncontact system and analyzed off-line following the procedure. A 12-lead ECG was obtained for each morphologically distinct VT induced. When a VT had left bundle branch block (LBBB) configuration, the combination of late inscription of the electrograms recorded at the RVA (and subsequent successful radiofrequency ablation of VT from a site within the LV) confirmed LV origin of the VT.

ECG Analysis

Surface ECG recordings for all VT were categorized by:

1. Bundle branch block (BBB) configuration
2. Inferior lead QRS complex polarity
3. Lead I QRS complex polarity
4. Lead aVL QRS complex polarity
5. Lead aVR QRS complex polarity
6. R-wave transition

BBB was defined as “left” or “right” based on QRS morphology in lead V1; right bundle branch block (RBBB) pattern was defined by a mono-, bi-, or triphasic R wave or qR in V1; LBBB pattern was defined by a QS, rS, or qRS in V1. The inferior leads were defined as ECG leads II, III, and aVF. Limb lead QRS complex polarity was defined according to the predominance of the QRS complex deflection being above (pos) or below (neg) the isoelectric line. In cases in which polarity of individual inferior leads differed, the polarity of the two leads in the same direction was selected. R-wave transition was defined as the ECG chest lead at which QRS polarity reversed (or recorded as concordant if absent). VT were defined as morphologically distinct if there was a difference in at least one of the criteria defined above.

Exit Site

VT exit site was defined as the point from which rapidly expanding endocardial systolic activation occurred on the

isopotential map synchronous with or just prior (up to 40 msec) to surface QRS onset (Fig. 1). High pass settings on the noncontact system were adjusted so that the smallest area of depolarization possible was observed. Virtual unipolar electrograms at all exit sites were analyzed to identify maximum negative dV/dt corresponding with the area of depolarization on the isopotential map. Epicardial mapping was not performed and, as such, VT exiting from a sub-epicardial site would not have been identified.

Location of Exit Site Region

In obtaining the 3-dimensional LV endocardial geometries, correct orientation was ensured using labels applied to confirm the positions of His and the orientation of the mitral annulus by bi-planar fluoroscopy. The geometries were then displayed in an “open” format with the map laid out after having been “cut” along the anterolateral border (Fig. 2). The maps were then divided into 9 regions of approximately equal area in a 3×3 grid format with regions categorized into basal, mid and apical in a longitudinal axis and septal, anterior, and posterior in a transverse axis (Fig. 2).

Evaluation and Statistical Methods

Positive predictive value (PPV) of a particular ECG pattern for an exit site region was defined as the percentage of VT exiting from a single region with the same ECG pattern, as a proportion of all VT with that ECG pattern. Only patterns with a PPV of $\geq 70\%$ were used to construct the algorithm, which was tested prospectively. Sensitivity was defined as the number of VT with the same ECG pattern and exit site as a proportion of all VT exiting from that region, expressed as a percentage. Sensitivity was not used as a criterion for inclusion in the algorithm.

Prospective Testing of the Algorithm

Eleven consecutive patients with 17 infarct-related VT undergoing noncontact mapping at a second center were enrolled into this part of the study. The algorithm was applied to 12-lead ECGs of VT by investigators blinded to noncontact mapping data.

Statistical Analysis

Further statistical validation of the algorithm was undertaken using a *k*-fold cross-validation method on all VT from both the retrospective and prospective limbs ($n = 138$) dividing these into three randomly selected equal subgroups ($n = 46$). The algorithm was then reconstructed using two of these subgroups, PPVs calculated for each ECG pattern generated and then applied to the remaining subgroup. This process was then repeated, using the alternative combinations of two subgroups.

Results

A total of 121 VTs were identified in 51 patients (mean 2.4 VT/patient), VTCL 391.7 ± 88.2 msec (range 227–600 msec), including 16 hemodynamically unstable (13%) and 12 nonsustained VT (9.9%). Thirty-eight patients had more than one morphologically distinct VT, including 19 patients in whom both LBBB and RBBB VT were identified. Seventy-nine VT had a RBBB pattern and 42 VT had a LBBB pattern. Previous infarction was anterior in 21 patients,

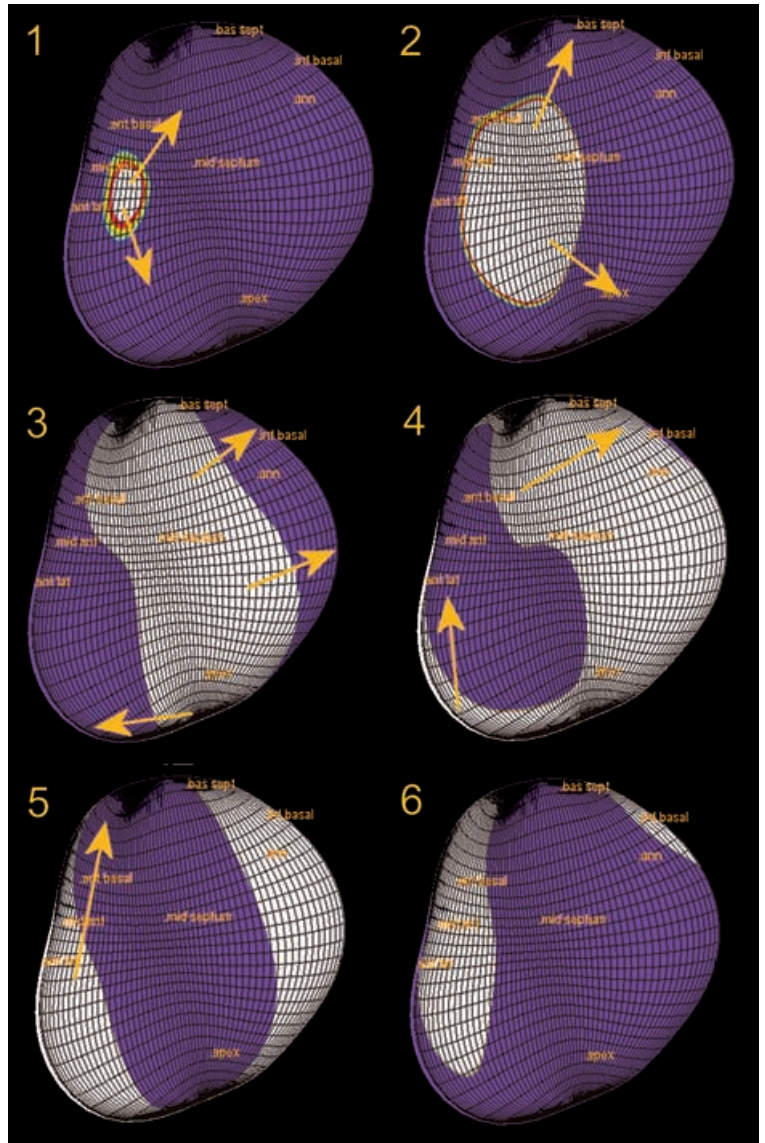


Figure 1. Isopotential map showing VT exit site and systolic activation pattern. Figure shows left ventricular endocardial isopotential maps opened out along the anterolateral wall. Purple indicates nondepolarized endocardium with other colors indicating depolarization with white being most negative areas. Yellow arrows indicate direction of wavefront propagation. The first map shows VT exiting from the mid-anterior wall, spreading septally and then posteriorly before arriving back to the mid-anterior wall region.

inferior in 17 patients, posterior in 5 patients, and multiple infarcts had occurred in 8 patients as determined by standard ECG criteria during normal sinus rhythm in combination with transthoracic echocardiography.

All patients with LBBB VT had infarction involving the septum. Noncontact mapping showed that all LBBB VT arose

from the septum, while all RBBB VT arose away from the septum.

Categorization of ECG Patterns

Using the specified ECG criteria, all VT could be categorized into a total of 10 distinct ECG patterns. Of these, 8

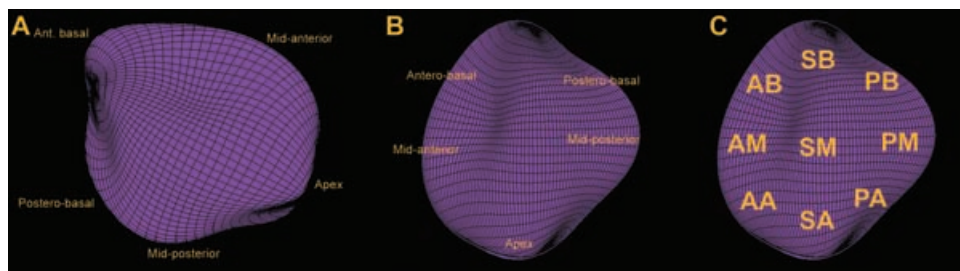


Figure 2. Figure showing how the noncontact isopotential maps were divided into 9 areas. A: The first panel shows the left ventricular endocardium in an RAO projection with anatomical positions marked. B: The same map is shown after being opened out along the antero-lateral border with the same anatomical positions. C: The third panel shows the same map as in panel 2 with all 9 anatomical positions marked. AA = antero-apical; AB = antero-basal; AM = mid-anterior; SA = apical septum; SB = basal-septum; SM = mid-septum; PA = posterior apex; PB = postero-basal; PM = mid-posterior.

TABLE 1

12-Lead ECG Patterns with Specificities or Sensitivities $\geq 70\%$ for VT Exit Site

	BBB	Inf. leads	I	aVL	aVR	Exit	PPV %	Sensitivity %
1	RBBB	neg	pos	pos		PM/PB	100	100
2	RBBB	neg	neg	neg		PA	100	18
3	RBBB	neg	neg	pos	pos	PA	77	59
4	RBBB	pos	neg	neg		AM	77	100
5	RBBB	pos	pos	neg		AB	100	100
6	LBBB	neg	neg			SB	100	33
7	LBBB	neg	pos	pos	neg	SM	100	35
8	LBBB	neg	pos	pos	pos	SA	22	100
9	LBBB	pos	neg			SM	100	22

AA = antero-apical; AB = antero-basal; AM = mid-anterior; BBB = bundle branch block; Exit = exit site; Inf. Leads = inferior lead polarity; LBBB = left bundle branch block; neg = negative polarity; PA = postero-apex; PM = mid-posterior; pos = positive polarity; PPV = positive predictive value; RBBB = right bundle branch block; SA = antero-septal; SM = mid-septum.

patterns had a PPV $\geq 70\%$ (Table 1), which accounted for 86 VT (71% of the total). A PPV $\geq 70\%$ was more common for RBBB than LBBB VT (60/79 [76%], vs 18/42 [43%]).

RBBB VT

Of the 79 RBBB VT identified, 48 (61%) had superior axes (negative polarity in the inferior leads) and 31 had inferior axes (positive polarity in the inferior leads). Five ECG patterns with PPV $\geq 70\%$ were identified correlating with

four exit site regions located in the postero-apical (PA), mid-anterior (AM), mid-posterior, or postero-basal (PM or PB), and antero-basal (AB) walls (Table 1). This accounted for 68 of the 79 RBBB VT identified (86%).

RBBB VT with a Superior Axis

RBBB VT with a superior axis accounted for the largest group of VT (n = 48) and correlated with three different exit site locations (Fig. 3A). Three ECG patterns had a PPV $\geq 70\%$, two correlating with a PA exit site (n = 13 and n = 4) and one to the PM or PB region (n = 27).

RBBB VT with an Inferior Axis

RBBB VT with an inferior axis correlated with four different exit sites: AM, PA, AA, and AB (Fig. 3B). VT arising from the AB and AM (n = 24) regions both had a PPV $\geq 70\%$, the latter accounting for all VT exiting from the AM region. Although there was only a single VT with an AB exit, this was the only example of a tachycardia exiting from that region (PPV 100%) and was therefore used in the algorithm construction.

LBBB VT

All LBBB VT were located in the septum. Of the 42 LBBB VT, 31 (74%) had a superior axis and 11 had an inferior axis. A total of 13 LBBB VT (31%) were associated with a PPV $\geq 70\%$.

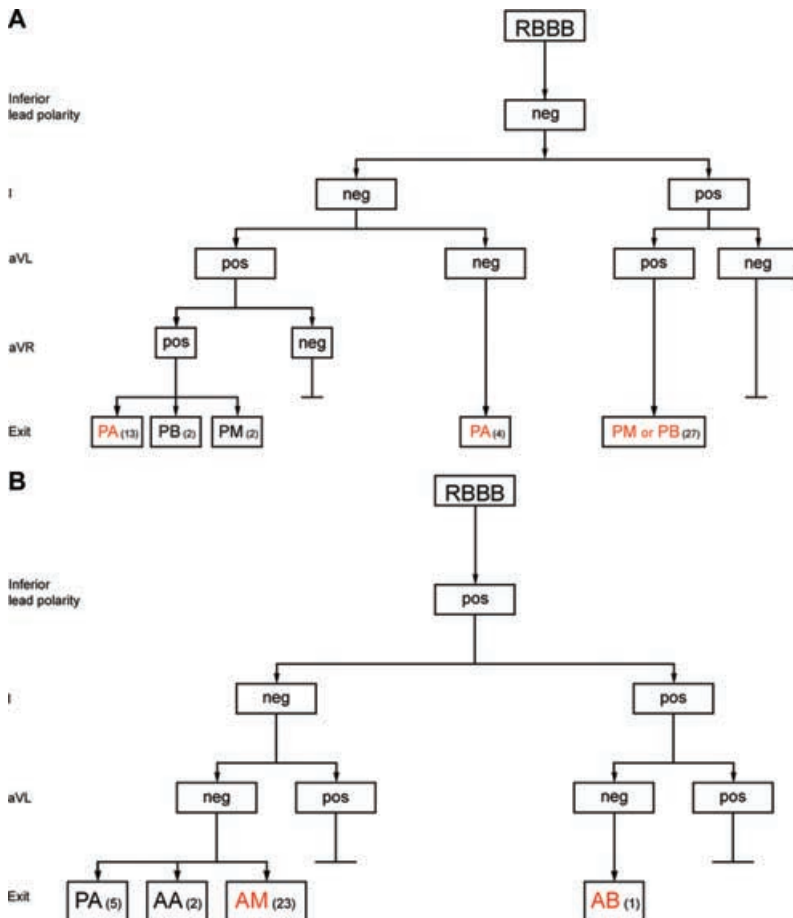


Figure 3. Algorithm correlating 12-lead ECG morphology of right bundle branch block (RBBB) VT with exit site region, derived from retrospective analysis. A: VT with negative (neg) polarity in the inferior leads. B: VT with positive (pos) polarity in the inferior leads. A vertical line ending a horizontal bar indicates no VT with this ECG pattern were identified. AA = antero-apical; AB = antero-basal; AM = mid-anterior; PA = postero-apical; PB = postero-basal; PM = mid-posterior. Exit sites with PPV $\geq 70\%$ are shown in red. Numbers of VT for each ECG pattern and exit site region identified in retrospective analysis are shown in brackets.

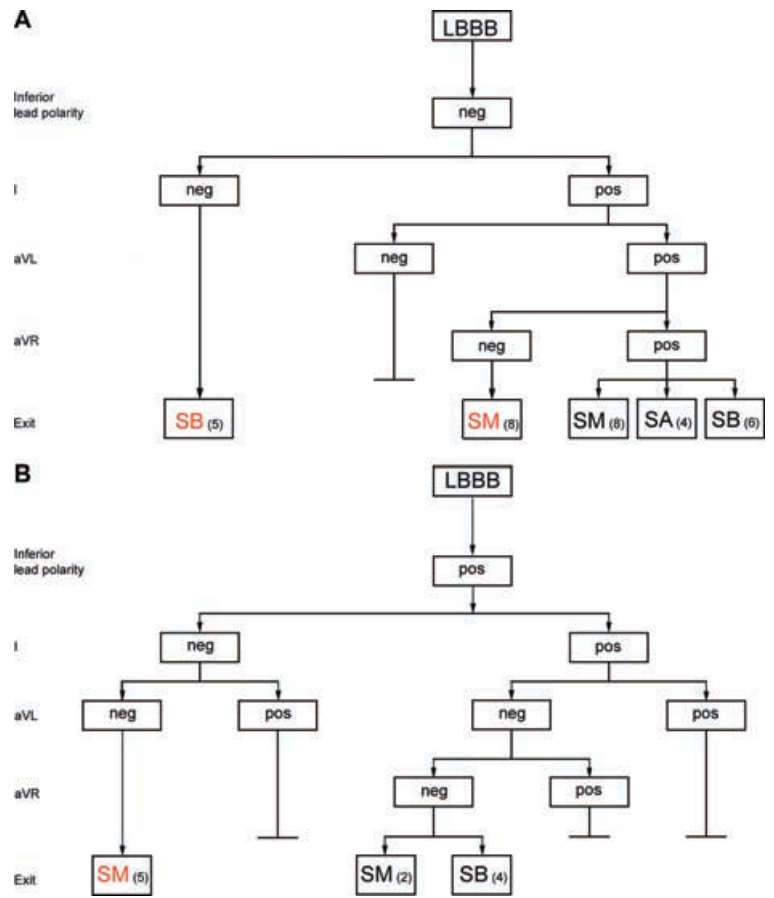


Figure 4. Algorithm correlating 12-lead ECG morphology of left bundle branch block (LBBB) VT with exit site region, derived from retrospective analysis. **A:** VT with negative (neg) polarity in the inferior leads. **B:** VT with positive (pos) polarity in the inferior leads. A vertical line ending a horizontal bar indicates no VT with this ECG pattern were identified. SA = antero-septal; SB = basal septum; SM = mid-septum. Exit sites with $PPV \geq 70\%$ are shown in red. Numbers of VT for each ECG pattern and exit site region identified in retrospective analysis are shown in brackets.

LBBB VT with a Superior Axis

LBBB VT with a superior axis correlated with two exit site locations, basal septum (SB) ($n = 5$) and mid-septal (SM) ($n = 8$; Fig. 4A), both with a PPV of 100%. LBBB VT with a superior axis and positive leads I, aVL, and aVR did not correlate with a specific exit site; however, all four VT exiting from the apical septum (SA) had this pattern (sensitivity 100%).

LBBB VT with Inferior Axis

LBBB VT with an inferior axis correlated with three exit sites of which one was significant, VT exiting from the mid-septum (SM) with a PPV 100% (Fig. 4B). The remaining 6 VT were located in the basal and mid-septum.

R-Wave Transition

Analysis of R-wave transition did not reveal any consistent or significant correlations and, as such, this ECG feature was not used in construction of the algorithm.

Prospective Analysis

A total of 17 VT were identified in 11 consecutive and unselected patients (3 female), mean age 53.5 ± 13.5 years, including 11 RBBB and 6 LBBB VT morphologies, with a mean cycle length of 368.9 ± 105.2 msec. Six patients had anterior infarction, three inferior infarction, one patient posterior infarction, and one patient both anterior and posterior infarction. Mean ejection fraction was $34.4 \pm 9.7\%$.

Application of the algorithm to the 12-lead ECGs of the VT morphologies prior to VT mapping predicted an exit site region with a $PPV > 70\%$ in 15 (88%). Of these, 14 (93%) were consistent with the exit site region determined by non-contact mapping. Details of these VT are shown in Table 2. The remaining VT arose from the mid-septum for which the algorithm had predicted a basal-septal exit site.

Validation of the Algorithm

Using the k -fold cross-validation method described above, positive predictive values for ECG patterns generated were not altered by the reduced size of the training set; and the performance of the rule was that in $84.3 \pm 4.9\%$ of cases in which the algorithm was able to predict an exit site, the correct region was identified.

Comparison of Algorithm with Previous Algorithms

Direct comparison between the algorithms from the present study and those of Miller et al. and Kuchar et al. is only possible for patients with anterior or inferior infarction, due to the limitations of the inclusion criteria of these earlier studies. Comparison of exit sites between these algorithms in the 10 patients in the prospective limb of the present study is presented in Table 3.

Using the algorithm developed by Miller et al. only six VT patterns yielded an exit site. Of these, none of them matched those predicted using the algorithm from the present study or the actual exit site located by noncontact mapping.

TABLE 2

Patient and ECG Characteristics, and Predicted and Actual Exit Sites for Prospectively Tested VT

Patient	Age	Sex	Infarct	EF%	VT	CL (ms)	BBB	Inf Leads	Lead I	Lead aVL	Lead aVR	Predicted Exit Site	Actual exit site	Correct
1	37	M	Ant	35	1	483	L	neg	pos	pos	pos	N/A	AA	N/A
					2	393	R	neg	pos	pos		PM	PM	Yes
2	38	F	Ant	40	1	443	L	pos	pos	neg	neg	SB	SB	Yes
3	61	F	Inf	20	1	455	R	pos	neg	neg		AM	AM	Yes
4	46	M	Inf	40	1	328	R	neg	neg	neg		PA	PA	Yes
5	53	M	Ant	15	1	429	L	pos	neg	neg		SM	SM	Yes
6	53	M	Ant	30	1	473	R	pos	neg	neg		AM	AM	Yes
					2	497	R	pos	neg	neg		AM	AM	Yes
					3	343	L	neg	pos	pos	pos	N/A	?	N/A
7	65	F	Ant	40	1	418	R	pos	neg	neg		AM	AM	Yes
					2	368	L	neg	pos	pos	neg	SM	SM	Yes
8	77	M	Inf	30	1	429	R	neg	neg	neg		PA	PA	Yes
9	58	M	Ant	40	1	200	R	pos	neg	neg		AM	AM	Yes
					2	222	L	neg	neg			SB	SB	Yes
					3	201	R	neg	neg	neg		PA	SB	No
10	66	M	Ant	35	1	280	R	neg	neg	pos	pos	PA	PA	Yes
11	35	M	Post	40	1	528	R	neg	neg	pos	pos	PA	PA	Yes

AA = antero-apical; AM = mid-anterior; Ant = anterior; BBB = bundle branch block configuration; CL = cycle length; Inf = inferior; Inf leads = polarity of inferior limb leads; N/A = Algorithm for this ECG pattern did not predict an exit site region with a PPV \geq 70%; PA = posterior apex; PM = mid-posterior; Post = Posterior; SB = basal septum; SM = mid-septum; VT = ventricular tachycardia; ? = VT exit site could not be clearly determined on noncontact isopotential map.

Using Kuchar et al.'s algorithm, an exit site was predicted for each VT pattern. Of these, the exit sites for eight VT exactly matched those predicted by the algorithm from the present study (accounting for five separate VT patterns). Of these, a single VT pattern (VT3 of patient 9) did not match the actual exit site located by noncontact mapping. In addition, Kuchar et al.'s algorithm predicted an exit site located adjacent to that of the present study and the actual exit, located by noncontact mapping.

Discussion

Despite the prognostic benefit of the implantable cardioverter-defibrillator (ICD),⁴⁻⁶ catheter ablation still pro-

vides a valuable role for patients with frequently symptomatic VT.⁷ This is especially important in patients with excessively frequent ICD therapies and in the 10–20% of patients who experience electrical storms,^{8,9} in whom ablation may be the only treatment option to avoid frequent shocks and in whom VT may be poorly tolerated, requiring rapid catheter placement to the region of interest.

Difficulties Localizing Areas of Importance in VT Circuits

Rapid localization of arrhythmogenic areas during conventional VT ablation is desirable to minimize time spent mapping during tachycardia, especially if poorly tolerated. When using conventional mapping techniques to map poorly

TABLE 3

Comparison of Predicted Exit Sites Using Algorithms from the Present Study and Those of Miller et al. and Kuchar et al. in Prospectively Tested Patients with Anterior or Inferior Infarction

Patient	Infarct	VT	Present Study	Miller et al.	Match	Kuchar et al.	Match	Actual Exit Site
1	Ant	1	N/A	Inf-apical septum	-	Inf-apical septum	-	AA
		2	PM	N/A	-	Mid-septal	No	PM
2	Ant	1	SB	N/A	-	Mid anterior	No	SB
3	Inf	1	AM	N/A	-	Basal antero-lateral	No	AM
4	Inf	1	AA	Inf-basal free wall	No	Mid-inferolateral	No	AA
5	Ant	1	SM	N/A	-	Central antero-apical	No	SM
6	Ant	1	AM	N/A	-	Mid-anterolateral	Yes	AM
		2	AM	N/A	-	Mid-anterolateral	Yes	AM
		3	N/A	Inf-apical septum	-	Mid-infero septal	-	?
7	Ant	1	AM	N/A	-	Central mid-anterior	Yes	AM
		2	SM	N/A	-	Basal infero-septal	Adjacent	SM
8	Inf	1	PA	Inf-basal free wall	No	Inferolateral apex	Yes	PA
9	Ant	1	AM	Ant-apical septum	No	Central/septal mid-anterior	Yes	AM
		2	SB	N/A	-	Mid basal septum	Yes	SB
		3	AA	Ant-apical septum	No	Central antero-apex	Yes (W)	SB
10	Ant	1	PA	N/A	-	Septal/central infero-apex	Yes	PA

"Match" refers to whether there was a match between the predicted exit site from the present study and that of Miller or Kuchar et al., respectively.

AA = antero-apical; Adjacent = predicted exit sites in adjacent regions; AM = mid-anterior wall; Ant = anterior; Inf = inferior; N/A = Algorithm did not predict an exit site for this pattern of VT; PA = posterior apex; PM = mid-posterior wall; SB = basal septum; SM = mid-septum; Yes (W) = match between predicted exit sites but both wrong.

tolerated VT, better localized mapping catheter placement before VT induction may permit exit site localization before immediate termination of the VT.

When voltage mapping is used, large areas of scar (up to 127 cm²)¹⁰ can be identified, from which it can be difficult to localize the precise regions critical for maintenance of a clinical VT. Thus, the use of an algorithm that can predict a region containing a VT exit site will reduce the area of the LV requiring detailed mapping and guide initial catheter placement, and possibly minimize the extent of empirical linear ablation between scar and anatomical structures.

Body surface mapping (BSM) has been used to identify sites of earliest activation during VT, but requires specialized equipment, and only 47% of endocardial breakthrough sites correlate with simultaneous endocardial mapping data.¹¹

Advances over Previous Algorithms

The algorithm constructed by Miller et al.¹ for VT exit site region localization was strictly limited to patients known to have had either “anterior” or “inferior” infarction (but not multiple infarcts). In addition, only sustained, hemodynamically stable VT was included in developing the algorithm that used conventional endocardial mapping (or epicardial mapping at surgery) to determine the exit site.

The algorithm of Kuchar et al. was also limited to patients with anterior and/or inferior infarction and used similar electrocardiographic features to our study to predict VT exit site location.² However, these characteristics were based on findings derived from ventricular pacing during sinus rhythm. The technique of pacemapping, although demonstrated to be logical and predictable in patients without wall motion abnormalities^{12,13} and accurate and specific when used in ablating idiopathic VT,^{14,15} has been shown to be less useful in guiding ablation for VT in the setting of structural heart disease.^{16,17} Furthermore, Waxman et al. demonstrated that pacing from sites only small distances away from the site of earliest activation could result in gross mismatches between ECGs recorded during VT and pacemapping.¹³

The exact location and anatomical distribution of infarct scar in patients is highly variable and, although often simply categorized as “anterior” or “inferior,” more specific infarct locations exist, e.g., infero-basal, postero-lateral, etc. Defining scar location using 12-lead ECG characteristics, LV angiography or echocardiography in patients with multiple infarcts may be difficult. Thus, by obviating the need for knowledge of infarct location, the algorithm in the present has greater clinical utility. It also has clear benefits in the patient with multiple or large zones of infarction in whom many LV areas could be candidates for VT initiation and potential targets for voltage-mapping guided ablation.

Furthermore, as we used ECG characteristics from episodes of VT rather than ventricular pacing, the algorithm we describe is likely to be more specific in patients with infarction than that of Kucher et al. The inclusion of nonsustained and rapid, hemodynamically unstable tachycardias in our analysis is an advance on both previous algorithms.

From our retrospective analysis, 64% of nonselected VTs were associated with a PPV \geq 70%, exceeding the 48% of highly selected VT identified in patients with single infarction of known territory in Miller et al.’s paper. A consistent finding among this present study and that of Miller et al. and Kucher et al. was that all LBBB VT arose from somewhere in the LV

septum. In contrast to Miller et al.’s paper, our study identified a higher proportion of RBBB VT with a PPV $>$ 70% than LBBB VT. This may be due to the greater proportion of RBBB VT than LBBB VT in our series.

The predictive accuracy of this algorithm (93%) is identical to that of Miller et al. (93%) and significantly better than the 39% of Kuchar et al. and has the advantage of not requiring subclassification based on infarct territory.

The inability to find any correlation between R-wave progression and/or transition and VT exit site region in our study is in direct contrast to both previously published algorithms. The reason for this difference is not clear but may relate to the nonselectivity of patients in our study, where both infarct location and VT cycle length were much more variable.

ECG Patterns Not Correlating to a VT Exit Site Region

Although the algorithm developed in this study identified 71% of VT with PPV \geq 70%, two ECG patterns failed to correlate specifically with an exit site region and both pertained to LBBB VT (Fig. 3C,D). As such, both could only correlate with three possible areas: the basal, mid, and apical septum. More detailed longitudinal discrimination using ECG limb lead polarity alone may not always be possible within the septum, or this may reflect a lack of numbers for these specific ECG patterns. Additionally, it may relate to the variability of infarct size and location between patients in the present study with subsequent effects on conduction patterns and manifest QRS for any given region of exit.

Limitations

Only 71% of VT identified were found to have a significant correlation with ECG morphology (PPV \geq 70%); thus, the algorithm is not universally applicable and cannot be used to determine exit sites for all VT. A correlation was said to exist if a PPV \geq 70% was found, even if the total number of VT were small and, in one case, where only a single VT exited from one region (antero-basal). This VT was used in the construction of the final algorithm although no VT exiting from the antero-basal region was tested prospectively and therefore its accuracy has not been evaluated. The value of 70% as a cutoff for PPV is arbitrary, a value over 80% would have excluded two correlations. The algorithm constructed in the present study is intended as a guide to exit sites for reentrant scar-related VT to enable more rapid localization and then mapping of the diastolic pathway in order to determine the best site for ablation. We have shown previously that the exit site per se is not the ideal site for ablation.³

Conclusions

The results of this study indicate that 12-lead ECG characteristics can reliably predict the LV VT exit site region in 71% of clinical VT without prior knowledge of infarct location. This method is not dependent on the sustainability of VT, can be applied over a wide range of cycle lengths and to patients with posterior and/or multiple sites of infarction. As such, this represents an incremental advance over previously published algorithms.^{1,2} This algorithm can be used in guiding initial placement of ablation catheters prior to VT initiation and mapping and may reduce procedural time during catheter ablation. It additionally offers the potential to facilitate a more focused and limited need for scar mapping, pacemapping, or

even transient entrainment mapping (and early termination) for unstable and nonsustained VT. Although the algorithm was prospectively evaluated in this study, its clinical utility in guiding ablation of infarct-related VT would need to be tested in a prospective study.

References

1. Miller JM, Marchlinski FE, Buxton AE, Josephson ME: Relationship between the 12-lead electrocardiogram during ventricular tachycardia and endocardial site of origin in patients with coronary artery disease. *Circulation* 1988;77:759-766.
2. Kuchar DL, Ruskin JN, Garan H: Electrocardiographic localization of the site of origin of ventricular tachycardia in patients with prior myocardial infarction. *J Am Coll Cardiol* 1989;13:893-903.
3. Schilling RJ, Peters NS, Davies DW: Feasibility of a noncontact catheter for endocardial mapping of human ventricular tachycardia. *Circulation* 1999;99:2543-2552.
4. A comparison of antiarrhythmic-drug therapy with implantable defibrillators in patients resuscitated from near-fatal ventricular arrhythmias. The Antiarrhythmics versus Implantable Defibrillators (AVID) Investigators. *N Engl J Med* 1997;337:1576-1583.
5. Moss AJ, Hall WJ, Cannom DS, Daubert JP, Higgins SL, Klein H, Levine JH, Saksena S, Waldo AL, Wilber D, Brown MW, Heo M: Improved survival with an implanted defibrillator in patients with coronary disease at high risk for ventricular arrhythmia. Multicenter Automatic Defibrillator Implantation Trial Investigators. *N Engl J Med* 1996;335:1933-1940.
6. Moss AJ, Zareba W, Hall WJ, Klein H, Wilber DJ, Cannom DS, Daubert JP, Higgins SL, Brown MW, Andrews ML: Prophylactic implantation of a defibrillator in patients with myocardial infarction and reduced ejection fraction. *N Engl J Med* 2002;346:877-883.
7. Segal OR, Chow AW, Markides V, Schilling RJ, Peters NS, Davies DW: Long-term results after ablation of infarct-related ventricular tachycardia. *Heart Rhythm* 2005;2:474-482.
8. Credner SC, Klingenhoben T, Mauss O, Sticherling C, Hohnloser SH: Electrical storm in patients with transvenous implantable cardioverter-defibrillators: Incidence, management and prognostic implications. *J Am Coll Cardiol* 1998;32:1909-1915.
9. Villacastin J, Almendral J, Arenal A, Albertos J, Ormaetxe J, Peinado R, Bueno H, Merino JL, Pastor A, Medina O, Tercedor L, Jimenez F, Delcan JL: Incidence and clinical significance of multiple consecutive, appropriate, high-energy discharges in patients with implanted cardioverter-defibrillators. *Circulation* 1996;93:753-762.
10. Marchlinski FE, Callans DJ, Gottlieb CD, Zado E: Linear ablation lesions for control of unmappable ventricular tachycardia in patients with ischemic and nonischemic cardiomyopathy. *Circulation* 2000;101:1288-1296.
11. van Dessel PF, van Hemel NM, de Bakker JM, Linnenbank TA, Potse M, Jessurun ER, SippensGroenewegen A, Wever EF: Relation between body surface mapping and endocardial spread of ventricular activation in postinfarction heart. *J Cardiovasc Electrophysiol* 2001;12:1232-1241.
12. Holt PM, Smallpeice C, Deverall PB, Yates AK, Curry PV: Ventricular arrhythmias. A guide to their localisation. *Br Heart J* 1985;53:417-430.
13. Waxman HL, Josephson ME: Ventricular activation during ventricular endocardial pacing: I. Electrocardiographic patterns related to the site of pacing. *Am J Cardiol* 1982;50:1-10.
14. Calkins H, Kalbfleisch SJ, el Atassi R, Langberg JJ, Morady F: Relation between efficacy of radiofrequency catheter ablation and site of origin of idiopathic ventricular tachycardia. *Am J Cardiol* 1993;71:827-833.
15. Klein LS, Shih HT, Hackett FK, Zipes DP, Miles WM: Radiofrequency catheter ablation of ventricular tachycardia in patients without structural heart disease. *Circulation* 1992;85:1666-1674.
16. Morady F, Harvey M, Kalbfleisch SJ, el Atassi R, Calkins H, Langberg JJ: Radiofrequency catheter ablation of ventricular tachycardia in patients with coronary artery disease. *Circulation* 1993;87:363-372.
17. Stevenson WG, Sager PT, Natterson PD, Saxon LA, Middlekauff HR, Wiener I: Relation of pace mapping QRS configuration and conduction delay to ventricular tachycardia reentry circuits in human infarct scars. *J Am Coll Cardiol* 1995;26:481-488.